Analyst

PAPER

View Article Online
View Journal | View Issue

Cite this: *Analyst*, 2017, **142**, 2500

Excellent peroxidase mimicking property of CuO/Pt nanocomposites and their application as an ascorbic acid sensor†

Xinhuan Wang, ‡[a] Qiusen Han, ‡[a,b] Shuangfei Cai,[a] Tian Wang,[a,b] Cui Qi,[a] Rong Yang *[a,b] and Chen Wang*[a,b]

Received 8th April 2017,
Accepted 24th May 2017

DOI: 10.1039/c7an00589j

rsc.li/analyst

Due to low cost and high stability, the applications of inorganic nanomaterials as efficient alternatives to natural enzymes are drawing much attention. In this work, novel CuO/Pt nanocomposites with high peroxidase-like activity were designed and applied for the colorimetric detection of ascorbic acid (AA). The nanocomposites were prepared by decorating Pt NPs on the surface of CuO nanosheets, which displayed good uniformity and showed improved distribution and stability. The catalytic activity of the prepared CuO/Pt nanocomposites was tested against various chromogenic substrates in the presence of H_2O_2, which displayed efficient peroxidase-like activity and high catalytic stability against temperature. The catalytic mechanism of the CuO/Pt nanocomposites was investigated by hydroxyl radical detection. The peroxidase-like activity decreased significantly in the presence of AA. On the basis of the inhibition property, a colorimetric biosensor was constructed by using the CuO/Pt nanocomposites for the detection of AA. It showed a high selectivity against amino acids, carbohydrates and normal ions. Thus, this work provides new insights into the application of inorganic nanocomposite-based nanozymes in the biosensing field.

1. Introduction

As a type of biological catalyst, enzymes are present in all organisms and involved in almost all reactions *in vivo* with high efficiency and specificity.[1,2] However, the secondary, tertiary, and quaternary structures of enzymes can be easily damaged by high temperature or chemical denaturants, which leads to a decrease or the loss of catalytic activity. Moreover, enzyme applications are also restricted by difficult preparation, high purification cost, and critical storage conditions. Therefore, it is more desirable to develop stable and efficient enzyme mimics for various applications.[3–5] The advances in nanoscience and nanotechnology have provided a new insight into the design and fabrication of enzyme mimics.

Inorganic nanomaterials as enzyme mimics have received increasing attention because of their several distinct properties, such as the abundance of reactive groups for further functionalization and more catalytic sites on their surfaces. Iron magnetic nanoparticles were first discovered with an intrinsic peroxidase-like activity similar to horseradish peroxidase (HRP).[6] Since the report, the design of functional nanomaterials with enzyme-like catalytic activity has attracted extensive attention.[7–15] Various nanomaterials, such as FeS nanoparticles,[16] V_2O_5 nanowires,[17] and Pt nanoparticles,[18] have been discovered with peroxidase-like activity. Cu species have a similar Fenton reactivity to Fe species, which is found to be associated with the peroxidase-like activity of Fe-based nanoparticles.[19] In addition, Cu is one of the cheapest metals and a precursor for copper oxides and metal-based nanomaterials. Furthermore, cupric oxide (CuO), a p-type semiconductor with a narrow band gap (1.2 eV), has been widely studied and applied in catalysis,[20] high temperature superconductors,[21] solar cells[22] and sensors.[23] The peroxidase-like activity of Cu-based nanomaterials has been studied.[24,25] Xia's group reported that CuO nanoparticles exhibited good peroxidase-like activity.[26] Thus, it is desirable to explore the enzymatic activity of CuO based nanomaterials.

Pt nanoparticles are one of the most important catalysts due to their excellent catalytic activity.[27] However, the catalytic activity of Pt nanoparticles is easily affected by the aggregation or the presence of capping agents. Two-dimensional (2D) layered materials like graphene or few-layer molybdenum disulfide (MoS_2) nanosheets, which have abundant active edges

[a]*CAS Center of Excellence for Nanoscience, National Center for Nanoscience and Technology, University of Chinese Academy of Sciences, Beijing 100190, P. R. China. E-mail: yangr@nanoctr.cn, wangch@nanoctr.cn*

[b]*Sino-Danish College, University of Chinese Academy of Sciences, Sino-Danish Center for Education and Research, Beijing, 100190, P. R. China*

†Electronic supplementary information (ESI) available. See DOI: 10.1039/c7an00589j

‡These authors contributed equally to this work.

and large surface areas, can provide support sites to load nanoparticles. Dong *et al.* synthesized graphene oxide–Fe_3O_4 magenetic nanocomposites with stable peroxidase-like activity.[28] However, to our knowledge, there are few reports focusing on the peroxidase-like activity of CuO/Pt nanocomposites and their application as biosensors.

Ascorbic acid (AA) is the main biological form of vitamin C, which participates in many biochemical functions as a cofactor for several enzymes.[29,30] Various methods have been developed for the detection of AA in recent years, including electrochemical,[31] spectrophotometric,[32] chromatographic,[33] and colorimetric methods. Due to its simplicity, rapidity, and low-cost, the colorimetric assay observed by the naked eyes has drawn increasing attention. On the basis of the antioxidant properties of AA, nano-peroxidase-based sensors are appealing for the detection of AA.[34]

Herein, we report a facile method to synthesize CuO/Pt nanocomposites as peroxidase mimics for the colorimetric detection of AA. Pt nanoparticles were well-dispersed on the surface of CuO nanosheets with high stability. The peroxidase-like activity of CuO/Pt was then confirmed with 3,3′,5,5′-tetramethylbenzidine (TMB), *o*-phenylenediamine (OPD) and 2,2′-azinobis(3-ethylbenzo-thiazoline-6-sulfonic acid) diammonium salt (ABTS) as chromogenic substrates. The reaction kinetics showed that CuO/Pt exhibited excellent peroxidase-like activity in comparison with HRP. On the basis of the antioxidant properties of AA, a fast and sensitive colorimetric method for AA detection was developed. This work explores a new CuO nanosheet-based peroxidase mimic with high catalytic activity for biosensing applications.

2. Materials and methods

2.1 Materials

Copper(II) chloride dihydrate ($CuCl_2{\cdot}2H_2O$), hexadecyltrimethyl ammonium bromide (CTAB) and *o*-phenylenediamine (OPD) were purchased from Alfa Aesar. 3,3′,5,5′-Tetramethylbenzidine (TMB) was bought from Acros. Chloroplatinic acid hexahydrate ($H_2PtCl_6{\cdot}6H_2O$) and 2,2′-azinobis(3-ethylbenzo-thiazoline-6-sulfonic acid) diammonium salt (ABTS) were obtained from J&K Scientific Ltd (Beijing, China). Terephthalic acid was bought from Sinopharm Chemical Reagent Co., Ltd (Shanghai, China). H_2O_2 was provided by Beijing Chemical Works (Beijing, China).

Other reagents and chemicals were at least analytical reagent grade. Ultrapure water was obtained by using a Milli-Q ultrapure system (18 MΩ cm).

2.2 Preparation of CuO nanosheets

CuO nanosheets were prepared *via* a hydrothermal method. Briefly, 0.5 g $CuCl_2{\cdot}2H_2O$ and 0.5 g CTAB were dissolved and mixed with 15 mL ultrapure water. Then, 1 mL (0.3 g mL^{-1}) sodium hydroxide (NaOH) aqueous solution was added into the mixture under vigorous stirring. Finally, the mixture was transferred to a 20 mL Teflon-lined stainless-steel autoclave and heated at 120 °C for 6 h. After being cooled to room temperature, the obtained materials were separated by centrifugation at 8000 rpm for 10 min, then washed with ultrapure water twice, and finally dispersed into ultrapure water.

2.3 Preparation of CuO/Pt nanocomposites

660 μL CuO nanosheet solution (170 mg L^{-1}) was dispersed in 2.34 mL water and sonicated for 10 min. 23.5 μL $H_2PtCl_6{\cdot}6H_2O$ aqueous solution (19.3 mM) was added. The mixture was stirred in an ice-water bath for 15 min. Then $NaBH_4$ (4.8 mM, 1 mL) aqueous solution was added into the mixture dropwise under vigorous stirring. After 2 h stirring, the resulting solution was centrifuged and washed three times. The obtained precipitate was re-dispersed in water before further characterization and application.

2.4 Characterization

Transmission electron microscopy (TEM) images were collected by using a transmission electron microscope (FEI Tecnai G2 20 S-TWIN). The analysis of the powder X-ray diffraction (XRD) spectrum was carried out on a D8 Advance X-ray diffractometer (Bruker, Germany). X-ray photoelectron spectra (XPS) were recorded by using an X-ray photoelectron spectrometer (Thermo Fisher ESCALAB 250Xi). The composition of the products was measured by using an energy dispersive spectra (EDS) detector.

2.5 Peroxidase-like catalytic activity evaluation

The peroxidase-like activity of CuO/Pt was assessed by the catalytic oxidation of TMB as the peroxidase substrate in the presence of H_2O_2. The reaction was carried out at room temperature in sodium acetate (NaOAC) buffer (0.2 M, pH = 4) using 2.5 μg CuO/Pt and H_2O_2 (1 mM) in the presence of TMB (1 mM), and the total reaction volume was 500 μL. The oxidation of TMB was evaluated by obtaining the absorption spectra at 652 nm using a UV-Vis spectrophotometer (PerkinElmer Lambda 950). The kinetic analysis of the peroxidase-like activity was performed at 40 °C with 4 μg CuO/Pt in NaOAC buffer (pH = 4.6) in the system of CuO/Pt–H_2O_2–TMB. The assay was carried out by varying the concentration of TMB with a constant concentration of H_2O_2 (5 mM) or varying the concentration of H_2O_2 with a constant TMB concentration (1 mM). The concentration of the oxidized TMB was quantified by using a molar absorption coefficient of ε = 39 000 M^{-1} cm^{-1}. The Michaelis–Menten constant was obtained based on the Lineweaver–Burk plots of the double reciprocal of the Michaelis–Menten equation:

$$\frac{1}{\upsilon} = \frac{K_m}{\upsilon_m}\left(\frac{1}{[S]} + \frac{1}{K_m}\right)$$

where υ is the initial velocity, υ_m represents the maximal reaction velocity, [S] is the concentration of the substrate and K_m is the Michaelis constant.

2.6 The investigation of catalytic reaction mechanism

To investigate the catalytic reaction mechanism, ·OH was evaluated by using terephthalic acid (TA) as a fluorescence probe in the CuO/Pt–H_2O_2 system, which was widely used for the detection of ·OH. 4 μg CuO/Pt and H_2O_2 (5 mM) were mixed at 40 °C in a total volume of 500 μL. TA (5 mM) solution was added and reacted for 30 min. The fluorescence spectrum was obtained by using a fluorescence spectrophotometer (PerkinElmer Lambda 950).

2.7 Colorimetric detection of ascorbic acid (AA)

The detection system was kept at a total volume of 500 μL. H_2O_2 (2 mM) and AA with different concentrations were mixed in NaOAC solution (0.2 M, pH = 4.6). Then, 3 μg CuO/Pt and TMB (1 mM) were added to the reaction system. The absorption spectra were obtained after 20 min of the reaction at 40 °C.

3. Results and discussion

3.1 Characterization of CuO/Pt nanocomposites

A schematic illustration of the synthesis of CuO/Pt nanocomposites is given in Fig. 1A. CuO nanosheets were first prepared *via* a hydrothermal synthesis method. The as-prepared CuO sheets could provide abundant anchor sites for Pt nanoparticles and could facilitate the formation of uniform Pt nanoparticles. Then, Pt nanoparticles were synthesized by $NaBH_4$ reduction using the CuO nanosheets as templates. Fig. 1B shows the catalytic properties of the CuO/Pt nanocomposites with TMB oxidation as a model reaction. A typical absorbance and a deep blue color could be observed, when TMB molecules were co-treated with CuO/Pt and H_2O_2. However, when AA was added, the oxidation of TMB was inhibited and the solution displayed a light blue colour. Moreover, the solution containing CuO/Pt and AA had no clear absorbance at 652 nm. Therefore, the nanocomposites with high peroxidase-like catalytic activity can be used for the detection of AA by a colorimetric method.

The morphology of the CuO/Pt nanocomposites was studied by using a transmission electron microscope (TEM). As shown in Fig. 2A, CuO exhibited a typical nanosheet structure with a smooth surface, and lots of homogeneous Pt nanoparticles were well formed on the surface of the CuO nanosheets. The average size of the Pt nanoparticles was less than 20 nm. The corresponding images of CuO nanosheets and Pt nanoparticles are shown in Fig. S1 and S2.† The synthesized CuO nanosheets were up to 2 μm in length and several tens of nm in width. The crystal structure of CuO/Pt was determined by X-ray diffraction (XRD) (Fig. 2B). The main diffraction peaks at 34.5°, 48.2°, 53.5° and 58.3° could be indexed to the (11−1), (20−2), (020) and (202) planes of CuO, and the peaks at 39.6° and 67.2° to the (111) and (220) planes of Pt. Energy dispersive X-ray spectroscopy (EDS) was performed for the elemental analysis of the CuO/Pt nanocomposites. From Fig. 2C, we can see the Cu, Pt and O signals of the sample. To further analyze the nature of the CuO/Pt nanocomposites, X-ray photo electron spectroscopy (XPS) was performed. In Fig. 2D and Fig. S3,† the peaks corresponding to Cu ($2p_{3/2}$), Cu ($2p_{1/2}$), O (1s), Pt ($4f_{5/2}$) and Pt ($4f_{7/2}$) could be seen in the spectra. The existence of satellite peaks in the spectra further confirmed that Cu existed in the sample as Cu^{2+}.[24] The survey spectrum revealed that Cu, Pt and O were present in the sample, which was consistent with the EDS analysis results. As shown in Fig. S4,† the zeta potentials of CuO nanosheets, Pt nanoparticles and CuO/Pt composites were 10.5 eV, −21.9 eV and −7.93 eV, respectively. The Pt nanoparticles could anchor on the surface of the CuO nanosheets through the electrostatic force. The above results indicated that the Pt nanoparticles were successfully fabricated on the surface of the CuO nanosheets.

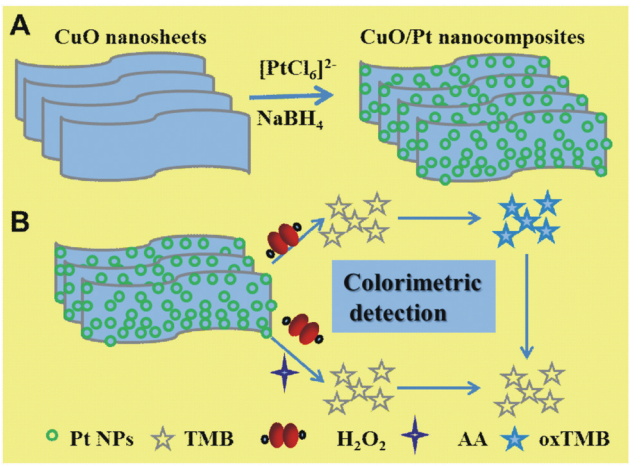

Fig. 1 Schematic illustration of (A) the synthesis of CuO/Pt nanocomposites and (B) CuO/Pt as peroxidase mimics with excellent peroxidase-like activity for highly selective colorimetric detection of ascorbic acid.

3.2 Peroxidase-like catalytic activity of CuO/Pt nanocomposites

As classical chromogenic substrates, 3,3′,5,5′-tetramethylbenzidine (TMB), 2,2′-azino-bis(3-ethylbenzothiazoline-6-sulfonic-acid) (ABTS) and *o*-phenylenediamine (OPD) were selected to investigate the peroxidase-like activity of the CuO/Pt nanocomposites in the presence of H_2O_2. As seen in Fig. 3A, all the three substrates were colorless; however, they displayed a typical color change upon the addition of CuO/Pt nanocomposites and H_2O_2. The TMB solution exhibited a deep blue color, the ABTS solution showed a green color and the OPD solution revealed a bright yellow color. The color changes indicated that the CuO/Pt exhibited the peroxidase-like activity. The enzymatic activities of CuO, Pt and CuO/Pt were further compared using TMB as a model substrate; H_2O_2 and buffer were applied as positive and negative controls, respectively, as shown in Fig. 3B. The CuO/Pt nanocomposites displayed the highest absorbance at 652 nm indicating the improved peroxidase-like catalytic activity. All materials were stable in solution

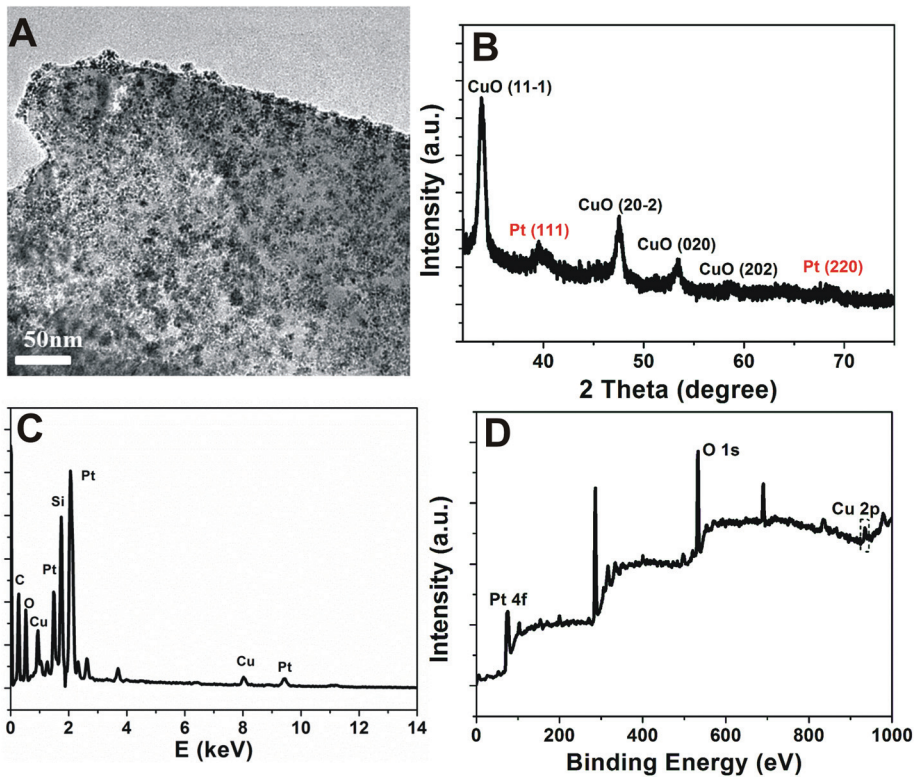

Fig. 2 (A) TEM image, (B) XRD pattern, (C) EDS spectrum, and (D) XPS full survey spectrum of the CuO/Pt nanocomposites.

at pH 4.5 (Fig. S5†), and the corresponding color changes of oxidized TMB are also shown in Fig. S6.† The highest enzyme mimicking activities can be ascribed to the synergistic effects of both the active sites of the Pt nanoparticles and the large surface area of the CuO nanosheets.

To optimize the catalytic reaction conditions, we further investigated the absorbance changes of the oxidized TMB with several important parameters, including pH, temperature and concentrations of CuO/Pt and H_2O_2 during the oxidation process of TMB (Fig. 4). The effects of pH and temperature were measured by varying the pH from 2 to 10 and the reaction temperature from 0 to 90 °C (Fig. 4A and B). The catalytic activities still remained high and stable when the reaction temperature was increased to 90 °C. The optimal conditions for the catalytic activities are a pH close to 4.6 and a temperature about 40 °C, respectively. Under the optimal conditions, the peroxidase activity was enhanced directly with the increasing concentration of H_2O_2 (Fig. 4C). Furthermore, a linear relationship was obtained between the absorbance of oxidized TMB and the CuO/Pt concentration at a constant concentration of H_2O_2, which suggested that the peroxidase mimicking activity was of first-order activity with respect to the CuO/Pt nanocomposites (Fig. 4D). The kinetics of the absorbance changes of oxidized TMB at 652 nm at different concentrations of the CuO/Pt nanocomposites are also shown (Fig. S7†).

The kinetic analysis of the CuO/Pt nanocomposites as a peroxidase mimic was further investigated using apparent steady-state kinetic experiments for the oxidation of TMB in the presence of H_2O_2. The kinetic data were obtained by using a series of TMB concentrations at a constant H_2O_2 concentration and *vice versa* (Fig. S8A and S8B†). The catalytic performance was fitted for the typical Michaelis–Menten model.[6] The Michaelis–Menten constant (K_m) and the maximum initial velocity (υ_{max}) were obtained from the Lineweaver–Burk double reciprocal plots, which showed a good linear relationship between υ^{-1} and $[S]^{-1}$ (Fig. S8C and S8D†).

It is known that K_m and υ_{max} are two crucial parameters to quantify the catalytic capacity of enzymes.[6] K_m represents the affinity of an enzyme to its substrate. The smaller the K_m values, the higher the affinity. υ_{max} indicates the reaction activity when an enzyme is saturated with the substrate. The apparent K_m and V_{max} values of CuO/Pt and HRP are listed in Table S1.† The K_m value of CuO/Pt with TMB as a substrate is smaller than that of HRP. A similar phenomenon is observed for H_2O_2 as a substrate when the results of CuO/Pt and HRP are compared. These results demonstrate that a lower concentration of TMB or H_2O_2 is required for CuO/Pt than HRP to achieve maximum activity. Moreover, the υ_{max} value of CuO/Pt with either TMB or H_2O_2 as a substrate is slightly better than that of HRP. Furthermore, the mechanism of the CuO/Pt peroxidase-like activity was investigated. It was assumed that CuO/Pt could decompose H_2O_2 and generate hydroxyl radicals, which could oxidize the substrate molecule. As a fluorescence probe to capture the hydroxyl radicals generated from the reaction, terephthalic acid (TA) was selected to evaluate the production of hydroxyl radicals during the reaction progress of

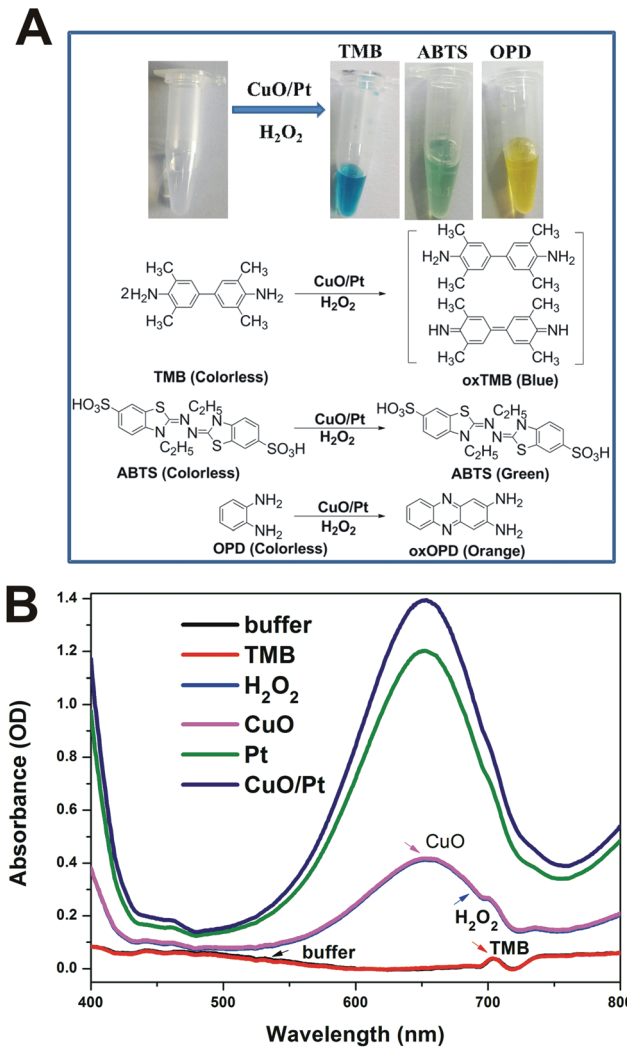

Fig. 3 (A) Color evolution of TMB, OPD and ABTS oxidation upon the addition of the CuO/Pt nanocomposites in the presence of H_2O_2. (B) UV-Vis absorption spectra of oxidized TMB treated with different samples.

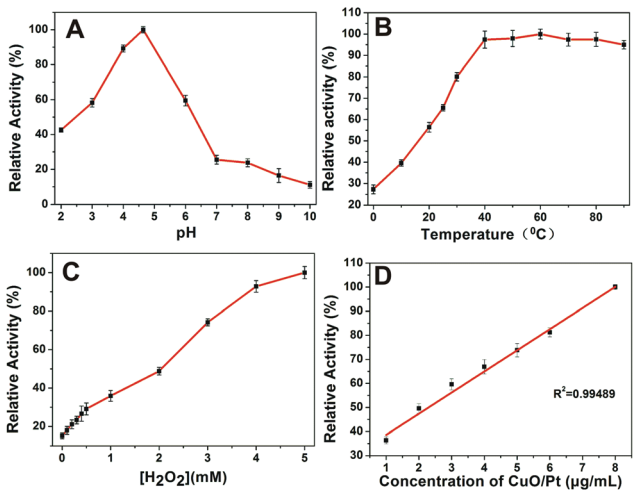

Fig. 4 Dependence of the peroxidase-like activity of CuO/Pt on (A) pH, (B) temperature, (C) H_2O_2 concentration and (D) CuO/Pt nanocomposite concentration.

CuO/Pt–H_2O_2.[2,35] TA itself is nonfluorescent, but it can easily react with the hydroxyl radicals to generate highly fluorescent 2-hydroxy terephthalic acid, which emits unique fluorescence around 435 nm. As shown in Fig. S9,† the remarkable enhancement of the fluorescence intensity was the evidence for the production of hydroxyl radicals by CuO/Pt in the presence of H_2O_2. The rise in fluorescence intensity was significant when compared with CuO/Pt in the absence of H_2O_2 or H_2O_2 alone. The results were consistent with the peroxidase-like activity of the CuO/Pt nanocomposites. The possible catalytic mechanism of the CuO/Pt nanocomposites might be ascribed to the generation of hydroxide radicals as shown in Fig. S10.†

3.3 Colorimetric detection of ascorbic acid

It is known that antioxidants can quench free radicals and inhibit their oxidation process. Among the radicals, hydroxyl radicals are known to be highly reactive species that rapidly oxidize the colorimetric substrate, such as TMB, during the H_2O_2-mediated oxidation reaction. Based on their peroxidase-like properties, CuO/Pt nanocomposites can be explored to detect antioxidants. Ascorbic acid (AA) is a well-known antioxidant and a form of vitamin C. In the current work, a colorimetric method was developed to detect AA, by using CuO/Pt nanocomposites.[32] CuO/Pt nanocomposites displayed peroxidase-like activity by generating hydroxyl radicals during the reaction process, which made it possible to detect AA. As shown in Fig. S11,† in the presence of H_2O_2, a typical absorbance and a deep blue color were observed with CuO/Pt and TMB in the solution. When AA was added, the oxidation of TMB was inhibited and the solution displayed a light blue color. Moreover, the solution containing CuO/Pt and AA did not show clear absorbance at 652 nm.

Therefore, a colorimetric method for the detection of AA was developed. Fig. 5A shows the absorbance of oxidized TMB responding to various concentrations of AA. In the presence of H_2O_2, the typical absorption peaks and a deep blue color of oxidized TMB could be observed for the solution containing CuO/Pt nanocomposites and TMB. Upon the introduction of both H_2O_2 and AA, the absorbance of the solution at 652 nm decreased. When the concentration of AA increased, the corresponding solution color changed from deep blue to colorless as shown in the inset of Fig. 5A. Therefore, AA-induced absorbance changes could be observed by the naked eyes. The corresponding absorbance changes *versus* concentrations of AA are presented (Fig. 5B). The absorbance changes displayed a good linear range from 1 μM to 0.6 mM. The limit of detection was estimated to be 0.796 μM (signal/noise = 3). Compared with other nanostructure-based detection methods for AA, the proposed colorimetric method not only showed a very comparable detection limit, but also provided a way to directly see AA-induced absorbance changes by the naked eyes. Furthermore, the detection method possessed the advantages of simple and low-cost detection procedures.[36] The kinetics of the absorbance changes of oxidized TMB at 652 nm were also shown in the system of CuO/Pt–H_2O_2–TMB with the addition of AA with different concentrations (Fig. S12†). The mechan-

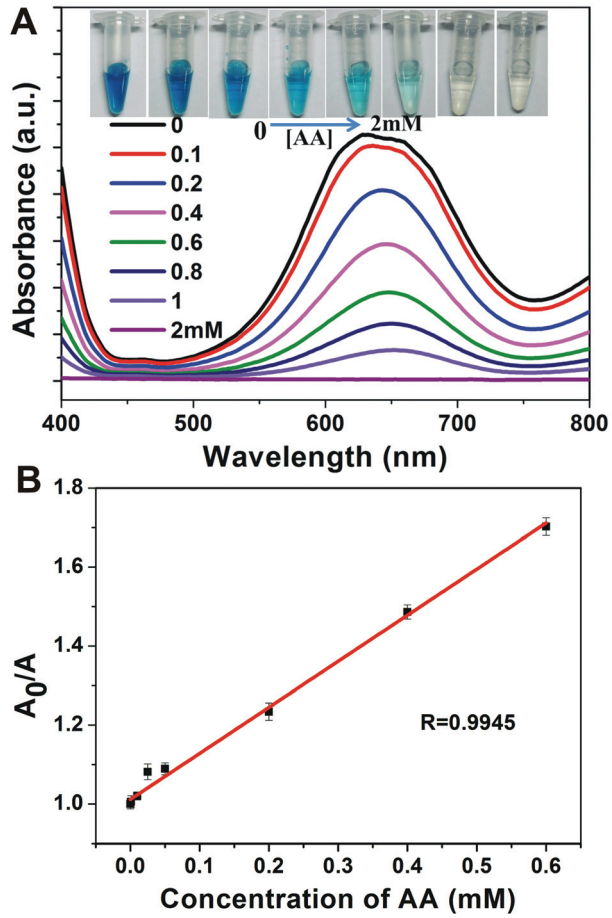

Fig. 5 (A) Effects of AA on the absorbance spectra of the TMB–CuO/Pt–H_2O_2 system. (Inset) Color changes of solutions with different concentration of AA. (B) Linear calibration plots of A_0 A^{-1} against AA concentrations. The LOD was calculated by the formula LOD = 3*S*/*K*, where *S* represents the standard deviation for a blank sample, and *K* is the slope of the calibration curve.

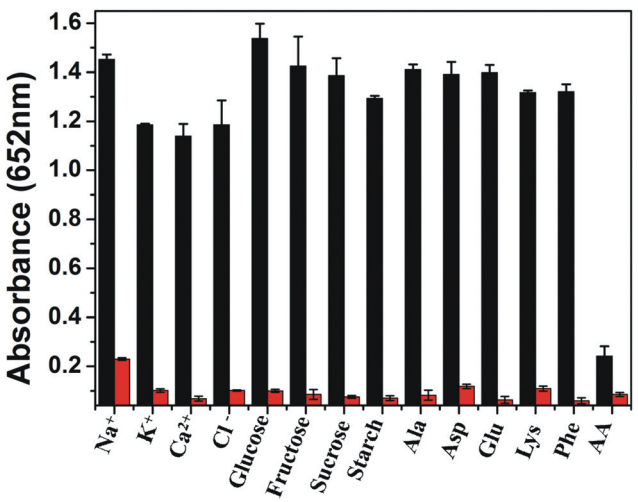

Fig. 6 Absorbance response of the TMB–CuO/Pt–H_2O_2 system to AA (2 mM) and interferential substances (2 mM). Black bars represent the addition of the interferential substance, and red bars represent the addition of interferential substance and AA together.

ism for the evaluation of the AA behavior can be understood. The hydroxyl radicals generated by H_2O_2 catalyzed by the CuO/Pt nanocomposites were quenched by AA, which led to the suppression of the TMB oxidation and resulted in a decrease of the absorbance at 652 nm (Fig. S13†).

The selectivity for AA detection was further investigated against amino acids, carbohydrates and normal ions in the system of CuO/Pt–H_2O_2–TMB. Fig. 6 shows the absorbance at 652 nm upon the addition of AA and other inferential substrates at the same concentration. Only the addition of AA caused the decrease in absorbance at 652 nm. Compared to the absorbance change with the addition of AA, no obvious inhibition effects were observed after the system was treated with inferential substrates alone. Therefore, the colorimetric assay based on CuO/Pt–H_2O_2–TMB in this study appears to be a useful method for AA detection.

4. Conclusions

In summary, we reported that CuO/Pt nanocomposites exhibited peroxidase-like activity against typical chromogenic substrates (TMB, OPD, and ABTS) in the presence of H_2O_2. The peroxidase-like activity was optimized by adjusting pH, temperature, H_2O_2 and CuO/Pt concentrations. The peroxidase-like activity behavior of CuO/Pt showed a typical Michaelis–Menten kinetics and good affinity to TMB and H_2O_2, indicating that CuO/Pt nanocomposites were efficient peroxidase-mimicking materials. A simple colorimetric method for AA detection using the CuO/Pt nanocomposites was developed. We believe that these results would be beneficial in the development of nanozymes for biomedical diagnosis, environmental monitoring and therapeutic applications.

Acknowledgements

This work was supported by the National key research and development program from the Ministry of Science and Technology of China (2016YFC0207102), the National Natural Science Foundation of China (21501034, 21573050, and 21503053) and the Chinese Academy of Sciences (XDA09030303). The financial support from the CAS Key Laboratory for Biological Effects of Nanomaterials and Nanosafety is also gratefully acknowledged.

Notes and references

1 S. Arya and S. Bhansali, *Chem. Rev.*, 2011, **111**, 6783–6809.
2 J. Mu, Y. Wang, M. Zhao and L. Zhang, *Chem. Commun.*, 2012, **48**, 2540–2542.
3 M. J. Wiester, P. A. Ulmann and C. A. Mirkin, *Angew. Chem., Int. Ed.*, 2011, **50**, 114–137.
4 Y. Huang, Z. Liu, C. Liu, E. Ju, Y. Zhang, J. Ren and X. Qu, *Angew. Chem., Int. Ed.*, 2016, **55**, 6646–6650.

5 P. Pessiki, S. Khangulov, D. Ho and G. Dismukes, *J. Am. Chem. Soc.*, 1994, **116**, 891–897.
6 L. Gao, J. Zhuang, L. Nie, J. Zhang, Y. Zhang, N. Gu, T. Wang, J. Feng, D. Yang, S. Perrett and X. Yan, *Nat. Nanotechnol.*, 2007, **2**, 577–583.
7 H. Wei and E. Wang, *Anal. Chem.*, 2008, **80**, 2250–2254.
8 S. Cai, C. Qi, Y. Li, Q. Han, R. Yang and C. Wang, *J. Mater. Chem. B*, 2016, **4**, 1869–1877.
9 S. Cai, Q. Han, C. Qi, Z. Lian, X. Jia, R. Yang and C. Wang, *Nanoscale*, 2016, **8**, 3685–3693.
10 Z. Yang, Y. Cao, J. Li, M. Lu, Z. Jiang and X. Hu, *ACS Appl. Mater. Interfaces*, 2016, **8**, 12031–12038.
11 Y. Song, X. Wang, C. Zhao, K. Qu, J. Ren and X. Qu, *Chem. – Eur. J.*, 2010, **16**, 3617–3621.
12 Q. Liu, Y. Yang, H. Li, R. Zhu, Q. Shao, S. Yang and J. Xu, *Biosens. Bioelectron.*, 2015, **64**, 147–153.
13 L. Sun, Y. Ding, Y. Jiang and Q. Liu, *Sens. Actuators, B*, 2017, **239**, 848–856.
14 Q. Liu, Y. Yang, X. Lv, Y. Ding, Y. Zhang, J. Jing and C. Xu, *Sens. Actuators, B*, 2017, **240**, 726–734.
15 L. Zhang, M. Chen, Y. Jiang, M. Chen, Y. Ding and Q. Liu, *Sens. Actuators, B*, 2017, **239**, 28–35.
16 Z. Dai, S. Liu, J. Bao and H. Ju, *Chem. – Eur. J.*, 2009, **15**, 4321–4326.
17 R. André, F. Natálio, M. Humanes, J. Leppin, K. Heinze, R. Wever, H. C. Schröder, W. E. G. Müller and W. Tremel, *Adv. Funct. Mater.*, 2011, **2**, 1501–1509.
18 G. W. Wu, S. B. He, H. P. Peng, H. H. Deng, A. L. Liu, X. H. Lin, X. H. Xia and W. Chen, *Anal. Chem.*, 2014, **86**, 10955–10960.
19 N. Wang, B. Li, F. Qiao, J. Sun, H. Fan and S. Ai, *J. Mater. Chem. B*, 2015, **3**, 7718–7723.
20 J. B. Reitz and E. I. Solomon, *J. Am. Chem. Soc.*, 1998, **120**, 11467–11478.
21 X. Zheng, C. Xu, Y. Tomokiyo, E. Tanaka, H. Yamada and Y. Soejima, *Phys. Rev. Lett.*, 2000, **85**, 5170–5173.
22 P. Poizot, S. Laruelle, S. Grugeon, L. Dupont and J. M. Tarascon, *Nature*, 2000, **407**, 496–499.
23 A. Chowdhuri, V. Gupta, K. Sreenivas, R. Kumar, S. Mozumdar and P. K. Patanjali, *Appl. Phys. Lett.*, 2004, **84**, 1180–1182.
24 A. P. Nagvenkar and A. Gedanken, *ACS Appl. Mater. Interfaces*, 2016, **8**, 22301–22308.
25 Y. Liu, G. Zhu, C. Bao, A. Yuan and X. Shen, *Chin. J. Chem.*, 2014, **32**, 151–156.
26 W. Chen, L. Hong, A. L. Liu, J. Q. Liu, X. H. Lin and X. H. Xia, *Talanta*, 2012, **99**, 643–648.
27 M. Ma, Y. Zhang and N. Gu, *Colloids Surf., A*, 2011, **373**, 6–10.
28 Y. Dong, H. Zhang, Z. Rahman, L. Su, X. Chen, J. Hu and X. Chen, *Nanoscale*, 2012, **4**, 3969–3976.
29 B. A. Eipper, D. A. Stoffers and R. E. Mains, *Annu. Rev. Neurosci.*, 1992, **15**, 57–85.
30 R. Salvatore De, C. Plinio, P. Antonella, S. Laura, P. Vito Di and C. Massimo, *Curr. Vasc. Pharmacol.*, 2010, **8**, 259–275.
31 V. Singh, P. C. Mondal, J. Y. Lakshmanan, M. Zharnikov and T. Gupta, *Analyst*, 2012, **137**, 3216–3219.
32 N. Malashikhina and V. Pavlov, *Biosens. Bioelectron.*, 2012, **33**, 241–246.
33 V. Gökmen, N. Kahraman, N. Demir and J. Acar, *J. Chromatogr., A*, 2000, **881**, 309–316.
34 A. Othman, A. Karimi and S. Andreescu, *J. Mater. Chem. B*, 2016, **4**, 7178–7203.
35 K. Ishibashi, A. Fujishima, T. Watanabe and K. Hashimoto, *Electrochem. Commun.*, 2000, **2**, 207–210.
36 H. Tan, C. Ma, L. Gao, Q. Li, Y. Song, F. Xu, T. Wang and L. Wang, *Chem. – Eur. J.*, 2014, **20**, 16377–16383.